EFFECTS OF CH_3COOH/H_2SO_4 MIXED-ACID HYDROLYSIS CONDITIONS ON THE YIELD AND PHYSICOCHEMICAL PROPERTIES OF CELLULOSE NANOCRYSTALS

MINGZE GAO,[*] XIAOPING GAO,[*,**,***] XIAORI YANG,[**] MIAO CHEN[**] and LIANHE LI[****]

[*]*College of Mechanics and Aeronautics, Inner Mongolia University of Technology, Hohhot, 010051, China*
[**]*College of Light Industry and Textiles, Inner Mongolia University of Technology, Hohhot, 010051, PR China*
[***]*Baotou Light Industry Vocational Technical College, Baotou, 014000, China*
[****]*College of Mathematics Science, Inner Mongolia Normal University, Hohhot, 010022, China*
✉ *Corresponding authors: X. Gao, gaoxp@imut.edu.cn*
X. Yang, yangxr0608@163.com.

Received August 3, 2026

In this study, cellulose nanocrystals (CNCs) were prepared from cellulose powder by CH_3COOH/H_2SO_4 mixed-acid hydrolysis. An L9(3^3) orthogonal design was used to evaluate the effects of acid ratio, temperature, and time on isolated CNC yield. The CH_3COOH/H_2SO_4 ratio showed the greatest main effect. Range analysis selected 90:10, 65 °C, and 90 min, for which the additive model predicted a yield of 92.93%; the confirmation experiment gave 87.90 ± 1.10% (n=3). CNC-4, prepared at 90:10, 55 °C, and 90 min, showed the highest measured yield among the original runs (88.52%). The CNCs exhibited rod-like morphology, with an average width of 50 ± 5 nm and length of 300 ± 50 nm, and relative crystallinity indices of 64.34-80.31%. FTIR and XPS supported the presence of carbonyl-containing ester groups and sulfur-containing surface species. Most CNC suspensions showed favorable aqueous dispersion stability, and CNC-4 exhibited slightly greater thermal resistance than SCNC.

Keywords: cellulose nanocrystals, CH_3COOH/H_2SO_4 mixed-acid hydrolysis, orthogonal experimental design, surface functionalization, aqueous dispersion stability

INTRODUCTION

Cellulose nanocrystals (CNCs) are rigid rod-like nanocrystals produced from natural cellulose by selectively removing the amorphous regions. They have high crystallinity, high specific surface area, excellent axial mechanical properties, and good biocompatibility. Their renewable origin and biodegradability further make them attractive for applications in high-performance nanocomposites, biomedical materials, water treatment, functional membranes, and coatings.[1-5] Preparation conditions strongly affect the particle dimensions, surface chemistry, crystallinity, colloidal stability, and thermal behavior of CNCs. Therefore, developing preparation routes that balance these characteristics remains an important research objective.

The main methods for preparing CNCs include acid hydrolysis, oxidation, enzymatic hydrolysis, ionic liquid/deep eutectic solvent treatment, and mechanochemical-assisted methods.[3,6,7] Acid hydrolysis remains one of the most widely used routes due to its well-established procedure, operational simplicity, and ability to produce highly crystalline CNCs.[8-10] Among acid hydrolysis systems, sulfuric acid hydrolysis is the most extensively studied. It selectively removes the amorphous regions of cellulose, while introducing a small number of sulfate half-ester groups onto the CNC surface, which improves the aqueous dispersion stability of the resulting nanocrystals.[8,9,11,12] Nevertheless, this process is highly sensitive to reaction conditions. Acid concentration, hydrolysis temperature, and reaction time strongly influence CNC yield, crystal dimensions, and surface charge. Accordingly, considerable efforts have been devoted to

improving CNC yield and properties by optimizing these parameters.[13,14] Chen *et al*.[10] examined the effects of processing parameters during concentrated sulfuric acid hydrolysis and found that, within the H_2SO_4 concentration range of 50-64 wt%, 58 wt% represented a critical threshold for high-yield CNC production. Below this concentration, partially hydrolyzed cellulose residues predominated, whereas above it, CNC yield increased markedly and reached approximately 70 wt% under suitable conditions. Roman *et al*.[12] further reported that sulfate half-ester groups, although beneficial for dispersion, substantially decrease the thermal stability of CNCs, thereby limiting their use in processes involving elevated temperatures. In addition, the use of large quantities of concentrated sulfuric acid presents practical challenges related to equipment corrosion, acid recovery, and wastewater treatment.[3]

To reduce sulfuric acid consumption, while retaining or improving the functional properties of CNCs, alternative hydrolysis systems based on phosphoric acid, organic acids, and mixed acids have been investigated.[6,7,15,16] Espinosa *et al.*[17] prepared phosphorylated CNCs from cotton fibers by phosphoric acid hydrolysis. The resulting CNCs exhibited better thermal stability than sulfated CNCs prepared by conventional sulfuric acid hydrolysis. Chen *et al*.[11] produced carboxylated CNCs and cellulose nanofibrils using recyclable organic acids, demonstrating that organic-acid hydrolysis can introduce functional groups onto cellulose surfaces through esterification. Du *et al*.[18] subsequently prepared thermally stable CNCs by $FeCl_3$-catalyzed formic acid hydrolysis, with reported yields exceeding 75%.

Mixed-acid systems have also attracted increasing interest because they can combine cellulose hydrolysis with surface modification.[19-21] Cheng *et al*.[19] prepared carboxylated CNCs using an H_2SO_4/HNO_3 mixed-acid system, while Xie *et al.*[20] used an H_2SO_4/oxalic acid system to obtain surface-functionalized CNCs with good aqueous dispersibility and improved thermal stability. More directly related to the present study, Wang *et al*.[21] demonstrated that sulfuric acid intensified acetic acid hydrolysis could produce functionalized CNCs at 80 °C using 5-10% H_2SO_4 and 70-90% acetic acid. The resulting CNCs exhibited rod-like morphologies, good dispersion stability, and improved thermal resistance, with a maximum reported yield of 81%. Although the feasibility of H_2SO_4-assisted acetic acid hydrolysis has already been established, the combined effects of the CH_3COOH/H_2SO_4 ratio, hydrolysis temperature, and reaction time on CNC yield and physicochemical properties require further clarification, particularly under relatively mild temperature conditions. In addition, the relationships among hydrolysis conditions, isolated yield, surface chemistry, crystalline structure, dispersion stability, and thermal degradation behavior have not been systematically examined within a single orthogonal experimental framework.

In this study, CNCs were prepared from cellulose powder by sulfuric acid catalyzed acetic acid hydrolysis. An L9(33) orthogonal experimental design was used to evaluate the effects of the CH_3COOH/H_2SO_4 volume ratio, hydrolysis temperature, and hydrolysis time on the isolated CNC yield. A confirmation experiment was subsequently conducted under the factor-level combination predicted by the range analysis. The morphology, surface chemistry, crystalline structure, aqueous dispersion stability, and thermal degradation behavior of the resulting CNCs were systematically characterized by scanning electron microscopy (SEM) and transmission electron microscopy (TEM), particle-size and zeta-potential measurements, Fourier-transform infrared spectroscopy (FTIR), X-ray photoelectron spectroscopy (XPS), X-ray diffraction (XRD), and thermogravimetric analysis (TGA). The objective of this work was to evaluate the effects of mixed-acid hydrolysis conditions on CNC yield and physicochemical properties and to identify a preferred preparation condition within the investigated range.

EXPERIMENTAL

Materials

H_2SO_4 (98 wt%) and CH_3COOH (99.5 wt%) were obtained from Tianjin Damao Chemical Reagent Co., Ltd. Cellulose powder was supplied by Shanghai Aladdin Biochemical Technology Co., Ltd. Dialysis tubing (MD44-1400D) was obtained from Hunan Bkmam Biotechnology Co., Ltd. All chemicals were of analytical grade and were used as received, without further purification.

Preparation of cellulose nanocrystals

Cellulose powder was dispersed in H_2SO_4/CH_3COOH mixed-acid solutions at a solid-to-liquid ratio of 1:40, and hydrolysis was performed under the designed conditions. The CH_3COOH/H_2SO_4 ratios reported in this study refer to the volume ratios of the as-received glacial acetic acid and sulfuric acid. The

CH_3COOH/H_2SO_4 volume ratio, hydrolysis temperature, and hydrolysis time were selected as the experimental factors for evaluating their effects on the isolated CNC yield. The CH_3COOH/H_2SO_4 volume ratios were 85:15, 90:10, and 95:5; the hydrolysis temperatures were 55, 65, and 75 °C; and the hydrolysis times were 30, 60, and 90 min. Each factor was evaluated at three levels, and the corresponding factor levels and L9(3^3) orthogonal experimental design are presented in Tables 1 and 2.

After hydrolysis, the reaction was immediately quenched by adding a tenfold volume of deionized water. The diluted mixture was allowed to stand at room temperature for 12 h. The clear supernatant was removed, and the lower white suspension was collected and centrifuged at 5500 rpm for 5 min. The acidic supernatant was discarded, and the precipitate was repeatedly washed with deionized water until a light-blue, opalescent suspension was obtained. The suspension was then transferred to dialysis tubing with a molecular-weight cutoff of 8000-14000 Da and dialyzed against deionized water until the pH of the dialysis medium remained neutral. The dialysis water was replaced every 12 h. The purified suspension was collected as the CNC suspension. An aliquot of the suspension was freeze-dried to determine the solid content and to provide dry material for subsequent characterization. The preparation procedure is illustrated in Figure 1. The samples prepared under the different orthogonal experimental conditions were designated CNC-1 through CNC-9, with the numerical suffix corresponding to the run number listed in Table 2.

A confirmation experiment was conducted under the factor-level combination predicted by the range analysis, namely a CH_3COOH/H_2SO_4 volume ratio of 90:10, a hydrolysis temperature of 65 °C, and a hydrolysis time of 90 min. Three independent batches were prepared under these conditions for determination of the isolated CNC yield.

For comparison, CNCs prepared by conventional sulfuric acid hydrolysis were used as the control. Cellulose powder was dispersed in a 64 wt% H_2SO_4 solution at a solid-to-liquid ratio of 1:40 and hydrolyzed at 45 °C under magnetic stirring for 60 min. The subsequent quenching, washing, centrifugation, dialysis, and freeze-drying procedures were performed as described above. The control sample was designated SCNC.

Statistical analysis and confirmation experiment

Range analysis was used to compare the effects of the experimental factors on the isolated CNC yield. For factor j at level *i*, K_{ji} represents the sum of the yields obtained at that level, whereas K_{ji} represents the corresponding mean yield. The range R_j was calculated as the difference between the maximum and minimum values of K_{ji}. A larger R_j value indicates a greater effect of the corresponding factor on the isolated CNC yield.

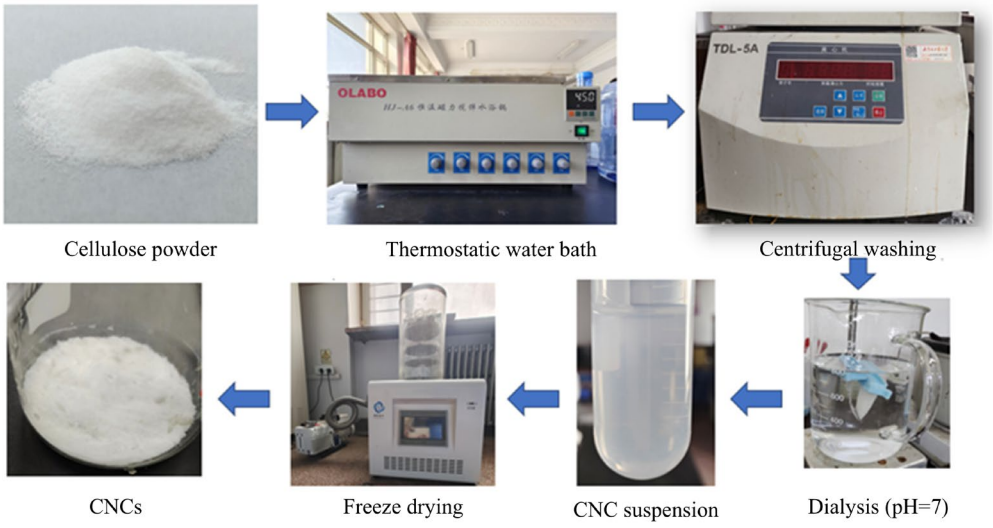


Figure 1: Preparation of CNCs via acid hydrolysis

Table 1
Orthogonal design table

Factor	Variable	Level		
CH_3COOH/H_2SO_4 volume ratio	A	85:15	90:10	95:5
Hydrolysis temperature (°C)	B	55	65	75
Hydrolysis time (min)	C	30	60	90

Table 2
L9 (3^3) Orthogonal experimental design

Run No.	A	B	C	CH_3COOH/H_2SO_4 volume ratio	Hydrolysis temperature	Hydrolysis time
1	1	1	1	85:15	55	30
2	1	2	3	85:15	65	90
3	1	3	2	85:15	75	60
4	2	1	3	90:10	55	90
5	2	2	2	90:10	65	60
6	2	3	1	90:10	75	30
7	3	1	2	95:5	55	60
8	3	2	1	95:5	65	30
9	3	3	3	95:5	75	90

The yield for the factor-level combination identified by the range analysis was estimated using an additive main-effects model:[22]

$$\hat{Y}_{ijk} = \overline{Y} + \left(\overline{Y}_{A_i} - \overline{Y}\right) + \left(\overline{Y}_{B_j} - \overline{Y}\right) + \left(\overline{Y}_{C_k} - \overline{Y}\right) \quad (1)$$

where $\hat{Y}_{ijk}$ is the predicted isolated CNC yield for the selected factor-level combination; $\overline{Y}$ is the overall mean yield of the 9 orthogonal experimental runs; $\overline{Y}_A, \overline{Y}_B$, and $\overline{Y}_C$ are the mean yields at the selected levels of factors A, B, and C, respectively. This model assumes that the contributions of the three main effects are additive and does not account for interactions among the factors.

A main-effects analysis of variance (ANOVA) was performed to evaluate the effects of the CH_3COOH/H_2SO_4 volume ratio, hydrolysis temperature, and hydrolysis time on the isolated CNC yield. A value of $p<0.05$ was considered statistically significant. Because interaction terms were not included in the statistical model, the ANOVA results were interpreted together with the range analysis and the confirmation experiment.

A confirmation experiment was performed using the factor-level combination selected on the basis of the range analysis. Three independent batches were prepared under the selected conditions, and the isolated CNC yield was reported as the mean ± standard deviation (n=3).

Characterization

Determination of CNC yield

A portion of the CNC suspension was freeze-dried and weighed to determine the CNC yield. The yield was calculated using the following equation:

$$Yield = \frac{V_2 \times m_1}{V_1 \times m_0} \times 100\% \quad (2)$$

where m_0 is the mass of the initial cellulose powder (g), m_1 is the dry mass of the freeze-dried aliquot (g), V_1 is the volume of the aliquot used for freeze-drying (mL), and V_2 is the total volume of the CNC suspension (mL).

Morphology and particle size of CNCs

The surface morphology of the samples was characterized using a Hitachi SU8220 scanning electron microscope (SEM) and an HT7700 transmission electron microscope (TEM). The particle size distribution and zeta potential of the CNC suspensions were determined using a Nanobrook 90Plus zeta potential and particle size analyzer.

Chemical and crystalline structure analysis of CNCs

XRD analysis was performed to investigate the crystalline structure of the samples. The XRD patterns were collected using Cu Kα radiation with a wavelength of 0.154 nm. The scanning range was 5°-40° in 2θ, with a step size of 0.02° and a scanning rate of 5°/min. The relative crystallinity of the samples was calculated using Equation (3):

$$C_{rI} = \frac{I_{200} - I_{am}}{I_{200}} \times 100\% \quad (3)$$

where C_{rI} is the relative crystallinity index (%), I_{200} is the diffraction intensity of cellulose at approximately 2θ =22.6°, corresponding to the (200) crystal plane of cellulose I, and represents the total scattering intensity from both crystalline and amorphous regions, I_{am} is the diffraction intensity at approximately 2θ =18°, representing the scattering intensity from the amorphous regions.

XPS was performed using a K-Alpha spectrometer to analyze the surface elemental composition of the CNCs, particularly the contents of C, O, and S. FTIR spectra were obtained using a Tensor spectrometer to identify the functional groups in the samples. The FTIR spectra were recorded over a wavenumber range of 400-4000 cm^{-1}.

Thermal stability of CNCs

The thermal stability of the samples was evaluated using an STA 449 F5 Jupiter simultaneous thermal analyzer. Approximately 10 mg of each sample was placed in a crucible and heated from 25 °C to 800 °C under a nitrogen atmosphere, at a heating rate of 10 °C/min.

RESULTS AND DISCUSSION

Effects of hydrolysis conditions on isolated CNC yield

Table 3 presents the isolated CNC yields obtained from the nine experimental runs and the corresponding range-analysis results. The range values followed the order A (25.05) > B (17.53) > C (10.48), indicating that the CH_3COOH/H_2SO_4 volume ratio had the greatest main effect on the isolated CNC yield within the investigated factor levels, followed by hydrolysis temperature and hydrolysis time. The highest mean yields were obtained at level 2 of factor A (82.50%), level 2 of factor B (76.04%), and level 3 of factor C (74.74%). Accordingly, the factor-level combination selected by the range analysis was $A_2B_2C_3$, corresponding to a CH_3COOH/H_2SO_4 volume ratio of 90:10, a hydrolysis temperature of 65 °C, and a hydrolysis time of 90 min.

Based on the additive main-effects model, the isolated CNC yield under the $A_2B_2C_3$ combination was predicted to be 92.93%. The confirmation experiment conducted under these conditions produced an isolated CNC yield of 87.90 ± 1.10% (n=3), which was approximately 5.03 percentage points lower than the predicted value. This discrepancy indicates that the additive model overestimated the isolated CNC yield, possibly because experimental variability and interactions among the factors were not independently represented in the model. Among the nine orthogonal experimental runs, CNC-4 exhibited the highest measured yield of 88.52%. This sample was prepared at a CH_3COOH/H_2SO_4 volume ratio of 90:10, a hydrolysis temperature of 55 °C, and a hydrolysis time of 90 min. The confirmation yield obtained at 65 °C was comparable to, but did not exceed, the yield of CNC-4 obtained at 55 °C. Thus, increasing the hydrolysis temperature from 55 to 65 °C did not improve the isolated CNC yield under the 90:10 mixed-acid ratio and 90 min hydrolysis time.

Table 3
Range analysis of CNC yield

Runs No.	A	B	C	CH_3COOH/H_2SO_4 volume ratio	Temperature	Hydrolysis time	Yield (%)
1	1	1	1	85:15	55	30	63.76
2	1	2	3	85:15	65	90	73.04
3	1	3	2	85:15	75	60	35.55
4	2	1	3	90:10	55	90	88.52
5	2	2	2	90:10	65	60	81.62
6	2	3	1	90:10	75	30	77.35
7	3	1	2	95:5	55	60	75.60
8	3	2	1	95:5	65	30	73.47
9	3	3	3	95:5	75	90	62.65
K_{j1}	172.35	227.88	214.58	—	—	—	—
K_{j2}	247.49	228.13	192.77	—	—	—	—
K_{j3}	211.72	175.55	224.21	—	—	—	—
$\bar{K}_{j1}$	57.45	75.96	71.53	—	—	—	—
$\bar{K}_{j2}$	82.50	76.04	64.26	—	—	—	—
$\bar{K}_{j3}$	70.57	58.52	74.74	—	—	—	—
R_j	25.05	17.53	10.48	—	—	—	—

Within the original L9 experimental matrix, $A_2B_1C_3$ therefore remained the highest-yielding tested combination. Because the original orthogonal runs were not independently replicated, however, this comparison should be regarded as descriptive rather than statistically conclusive.

For comparison, SCNC prepared by conventional sulfuric acid hydrolysis exhibited an isolated yield of 25.84%, whereas CNC-4 yielded 88.52% in the corresponding orthogonal experimental run. Under the experimental conditions used in this study, the selected mixed-acid condition therefore resulted in a higher isolated CNC recovery than the conventional sulfuric acid control. Previous studies have demonstrated that CNC yield is sensitive to the cellulose source and hydrolysis parameters, including acid concentration, acid-to-cellulose ratio, reaction temperature, and hydrolysis time.[25,26] Therefore, the present comparison should be interpreted within the specific experimental conditions of this study rather than as a general

difference between mixed-acid and conventional sulfuric acid hydrolysis processes. In contrast, CNC-3 exhibited the lowest isolated yield of 35.55% at a CH_3COOH/H_2SO_4 volume ratio of 85:15, a hydrolysis temperature of 75 °C, and a hydrolysis time of 60 min. The low recovered yield may reflect intensified cellulose hydrolysis and degradation under the combined effects of a relatively high sulfuric acid proportion and elevated temperature. Under these conditions, a greater fraction of the cellulose may have been converted into soluble degradation products that were removed during washing and dialysis. Nevertheless, because interactions among the experimental factors were not independently evaluated, the low yield cannot be attributed to any single factor alone.

Table 4 summarizes the main-effects ANOVA results. The p-values obtained for the CH_3COOH/H_2SO_4 volume ratio, hydrolysis temperature, and hydrolysis time were 0.015, 0.017, and 0.035, respectively. All three values were below the significance threshold of 0.05, and the magnitude of the corresponding F-values was consistent with the ranking obtained from the range analysis. However, the residual error had only two degrees of freedom because the L9 experimental runs were not independently replicated and interaction terms were not included in the model. The ANOVA results should therefore be interpreted as exploratory evidence of main effects rather than definitive statistical confirmation.

Table 4
ANOVA results of CNC yield

Parameter	Type III sum of squares	Degrees of freedom	Mean square	*F*-value	p-value
Corrected model	1853.401a	6	308.900	57.358	0.017
Intercept	44318.670400	1	44318.670	8229.248	0.000
A	941.723	2	470.862	87.431	0.015
B	704.696	2	352.348	65.425	0.017
C	300.217	2	150.108	27.873	0.035
Error	10.771	2	5.386	—	—
Total	46182.842	9	—	—	—
Corrected total	1864.172	8	—	—	—

Aqueous dispersion stability and zeta potential of CNCs

Figure 2 shows photographs of 1 wt% CNC suspensions immediately after ultrasonication and after 15 days of standing. Immediately after ultrasonication, all CNC suspensions appeared visually homogeneous in deionized water. After 15 days, slight sedimentation was observed for CNC-1 and CNC-9, whereas no obvious sedimentation was observed for the other samples. The whitish sediments may have originated from incompletely hydrolyzed cellulose fragments and particle aggregates, although their composition was not independently determined.

Table 5 presents the zeta potentials of the CNC suspensions. In general, a greater zeta-potential magnitude is associated with stronger electrostatic repulsion between suspended particles and a lower tendency toward aggregation.[23] Except for CNC-1 and CNC-9, the CNC samples exhibited zeta potentials of approximately -30 to -40 mV, indicating substantial negative electrokinetic potentials. These negative potentials can promote electrostatic repulsion between particles and thereby contribute to suspension stability. In comparison, CNC-1 and CNC-9 exhibited lower zeta-potential magnitudes, with values of -26.91 ± 2.42 and -23.61 ± 2.34 mV, respectively. These results are consistent with the slight sedimentation observed for the two samples after 15 days. The negative zeta potentials of the CNC suspensions are consistent with the presence of anionic surface groups introduced during mixed-acid hydrolysis, particularly sulfate-containing groups derived from sulfuric acid. Acetyl-containing groups may also influence CNC-water and CNC-CNC interactions by altering surface hydrophilicity and interparticle hydrogen bonding. However, their specific contribution to the dispersion stability cannot be determined from the zeta-potential measurements alone.

CNC-2 through CNC-8 generally exhibited greater zeta-potential magnitudes than CNC-1 and CNC-9, suggesting that the hydrolysis conditions

were associated with differences in the interfacial charge and dispersion behavior of the resulting CNCs. The sedimentation observed for CNC-1 may be related to incomplete hydrolysis under the relatively low temperature and short reaction time, whereas that observed for CNC-9 may be associated with aggregation or the presence of larger particles after prolonged hydrolysis at an elevated temperature. These explanations remain tentative because the composition and particle-size distribution of the sediments were not separately analyzed. CNC-4 through CNC-8 were subsequently subjected to hydrodynamic-size analysis, whereas CNC-4 through CNC-6 were selected for electron-microscopy observations.

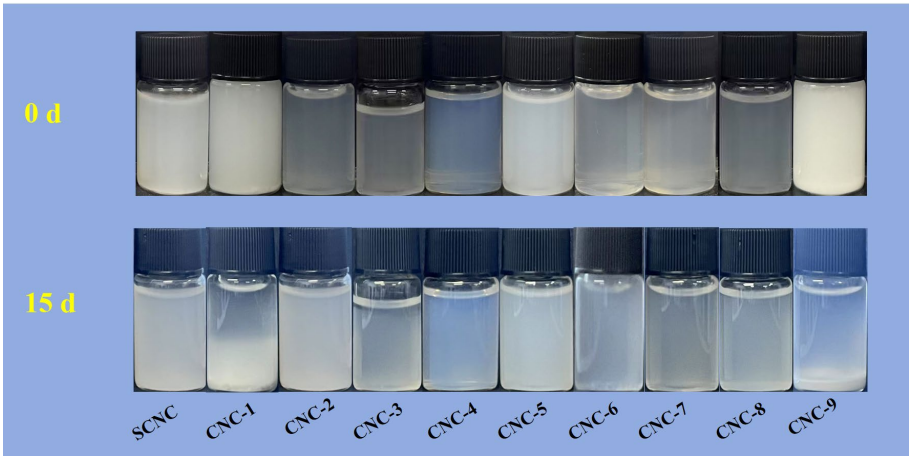


Figure 2: Dispersion stability of 1 wt% CNC suspensions in water after standing for 0 and 15 days

Table 5
Zeta potentials of CNC samples

Sample	Zeta potential (mV)
SCNC	-30.53 ± 3.21
CNC-1	-26.91 ± 2.42
CNC-2	-35.61 ± 2.65
CNC-3	-31.82 ± 2.14
CNC-4	-34.61 ± 1.23
CNC-5	-34.23 ± 4.12
CNC-6	-32.53 ± 2.14
CNC-7	-35.31 ± 2.31
CNC-8	-33.23 ± 1.34
CNC-9	-23.61 ± 2.34

Hydrodynamic size and morphology of CNCs

Figure 3 shows the hydrodynamic size distributions of the representative CNC suspensions. The predominant size populations of CNC-4, CNC-5, CNC-6, CNC-7, and CNC-8 were distributed within approximately 100-400 nm. Among these samples, CNC-6 exhibited a relatively narrow and concentrated distribution, suggesting greater size uniformity in suspension. CNC-4 and CNC-5 also showed relatively concentrated distributions, with their predominant populations occurring within 100-300 nm. In comparison, CNC-7 and CNC-8 exhibited broader distributions extending to approximately 400 nm, indicating greater size heterogeneity and particle association in suspension. Overall, the particle-size analysis showed that the selected CNC suspensions contained particles with hydrodynamic sizes in the nanometer range.

Figure 4 shows the SEM image of cellulose powder and the TEM images of the CNC samples after hydrolysis. As the starting cellulose material, cellulose powder contains both crystalline and amorphous regions and exhibits a rod-like morphology, with an average diameter of approximately 25 μm and an average length of approximately 100 μm. CNC-4, CNC-5, and CNC-6 were selected for TEM observation because they exhibited good dispersion stability and relatively concentrated particle size distributions, making

them representative samples for morphological analysis. After hydrolysis, the obtained CNCs displayed a nanoscale rod-like morphology, with an average diameter of 50 ± 5 nm and an average length of 300 ± 50 nm. These dimensions are broadly consistent with the particle size distribution results, further confirming the formation of nanoscale cellulose crystals.

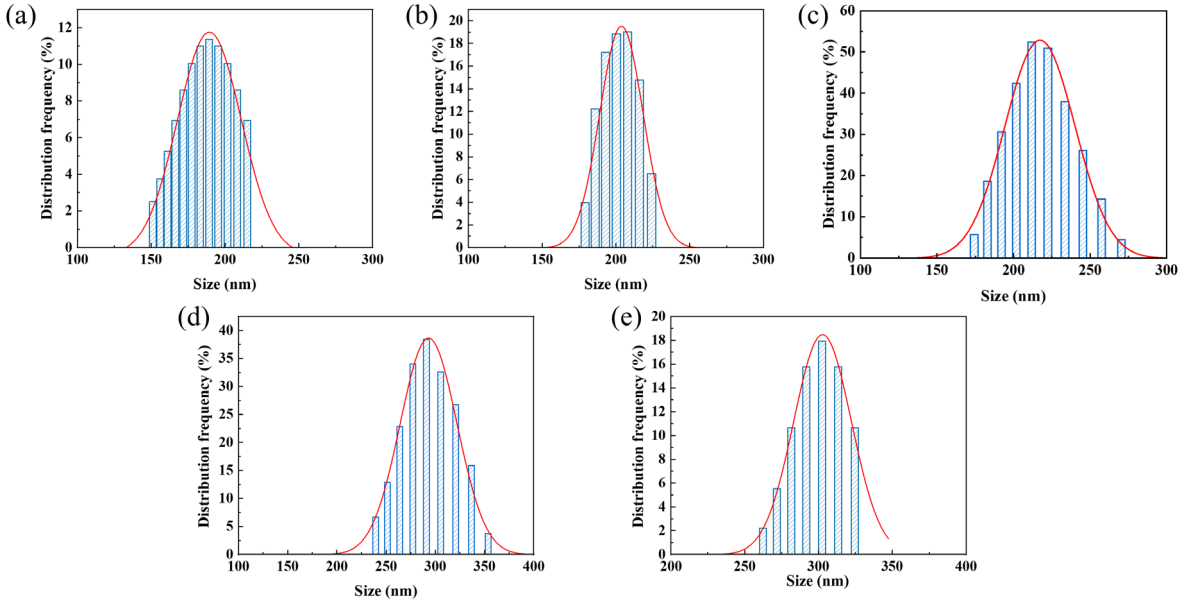


Figure 3: Particle size distributions of representative CNC samples (a) CNC-4, (b) CNC-5, (c) CNC-6, (d) CNC-7, (e) CNC-8

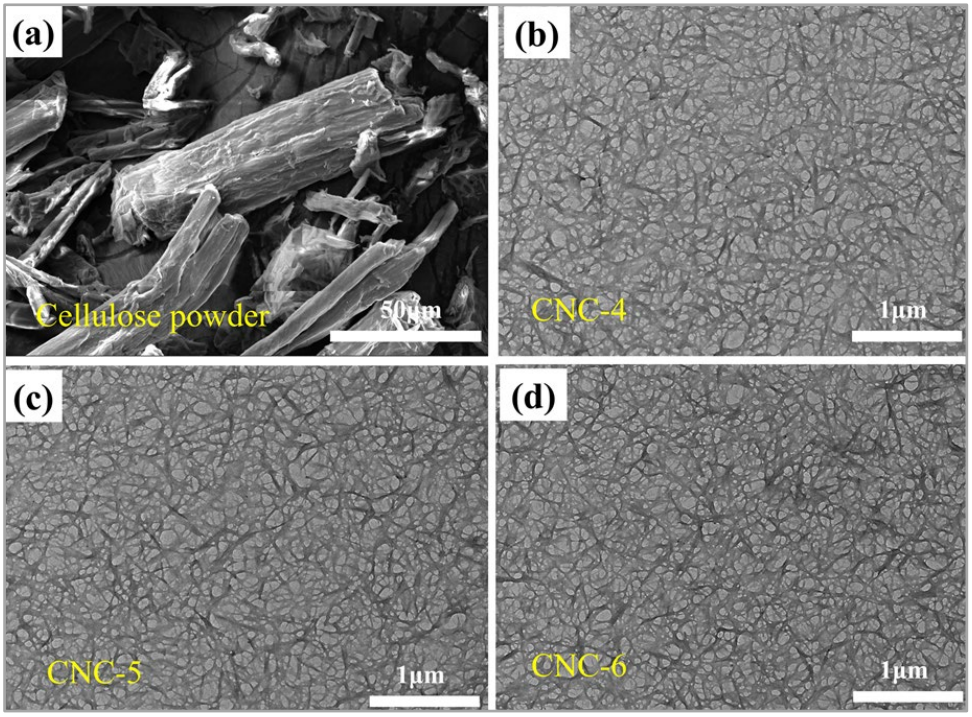


Figure 4: SEM image of cellulose powder (a) and TEM images of representative CNC samples (b-d)

Chemical structure, surface composition, and crystalline structure of CNCs

The chemical structure and surface elemental composition of the samples were investigated by FTIR and XPS, respectively. Figure 5(a) shows the FTIR spectra of cellulose powder, SCNC, and CNC-4. Compared with cellulose powder and SCNC, CNC-4 exhibited an additional absorption

band at 1741 cm^{-1}, which was assigned to the C=O stretching vibration of ester carbonyl groups. The appearance of this band is consistent with the formation of acetyl-containing ester groups during mixed-acid hydrolysis. The three samples exhibited similar absorption bands at 3392, 2900, 1637, 1370, 1057, and 890 cm^{-1}. The bands at 3392 and 2900 cm^{-1} were assigned to O-H and C-H stretching vibrations, respectively, whereas the band at 1637 cm^{-1} was associated with the bending vibration of adsorbed water molecules. The bands at 1370 and 1057 cm^{-1} were attributed to C-H bending and C-O/C-O-C stretching vibrations, respectively, while the band at 890 cm^{-1} was associated with the β-glycosidic linkages of cellulose. The retention of these characteristic bands indicates that the cellulose backbone was largely preserved after acid hydrolysis. The characteristic vibrations of sulfate-containing groups generally occur in the range of approximately 1000-1350 cm^{-1}. However, this region overlaps substantially with the C-O and C-O-C vibrations of cellulose, particularly the band near 1057 cm^{-1}. Therefore, the presence of sulfur-containing surface groups could not be conclusively determined from the FTIR spectra alone.

Figure 5(b) shows the XPS survey spectrum of CNC-4, in which signals corresponding to C, O, and S were detected. The detection of the S2p signal supports the presence of sulfur-containing species on the CNC surface following sulfuric-acid-assisted hydrolysis. CNC-4 was selected as the representative sample for XPS analysis because it exhibited the highest measured yield among the nine orthogonal experimental runs and good aqueous dispersion stability. Figure 5(c) shows its high-resolution C1s spectrum, which was deconvoluted into three main components centered at 284.8, 286.8, and 288.3 eV. These components were assigned to C-C/C-H, C-O, and C=O/O-C=O bonding environments, respectively. The component at 288.3 eV was consistent with the carbonyl absorption band observed at 1741 cm^{-1} in the FTIR spectrum. Taken together, the FTIR and XPS results support the presence of carbonyl-containing ester groups on the CNC-4 surface.

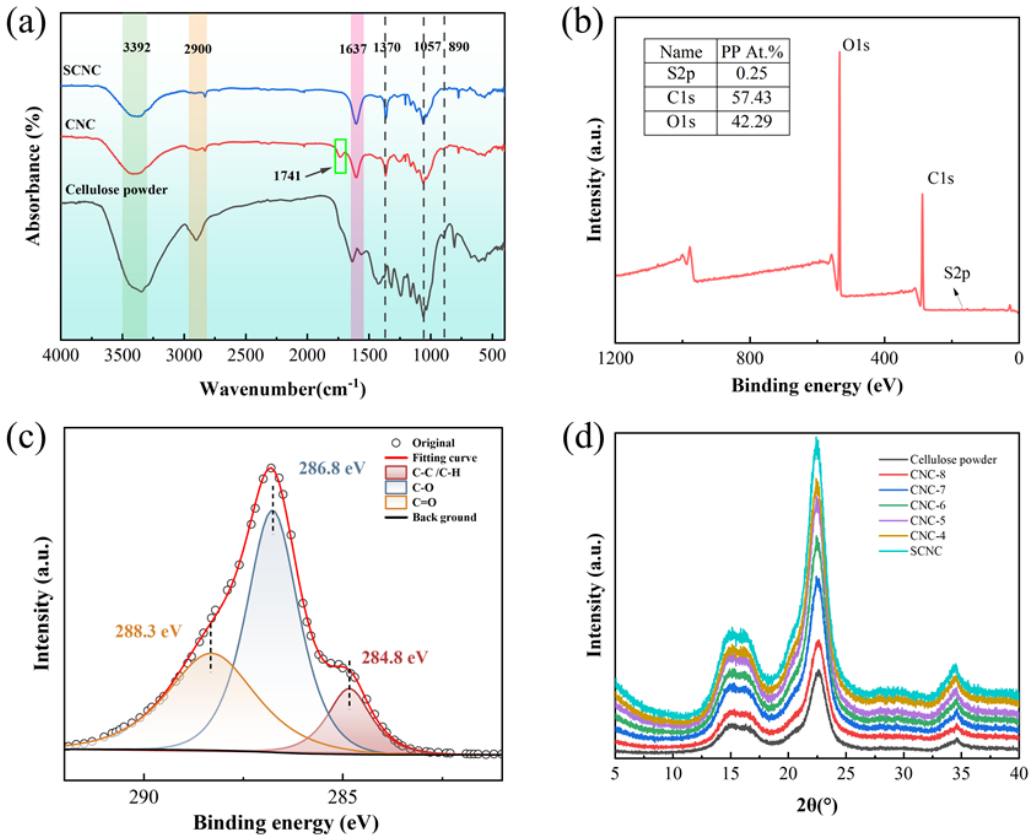


Figure 5: FTIR, XPS, and XRD analyses of cellulose powder, SCNC, and CNCs; (a) FTIR spectra, (b) XPS survey spectrum, (c) high-resolution C1s XPS spectrum, (d) XRD patterns

Table 6
Crystallinity of cellulose powder, SCNC, and CNC samples

Sample	Crystallinity (%)
Cellulose powder	60.83
SCNC	79.72
CNC-4	80.31
CNC-5	78.52
CNC-6	75.32
CNC-7	70.51
CNC-8	64.34

Figure 5(d) shows the XRD patterns of cellulose powder, SCNC, and CNC-4 through CNC-8. All samples exhibited diffraction peaks at approximately 2θ=15.1°, 16.5°, 22.6°, and 34.6°, corresponding to the ($1\bar{1}0$), (110), (200), and (004) planes of cellulose I, respectively. The retention of these characteristic diffraction peaks indicates that the cellulose I crystalline structure was preserved after mixed-acid hydrolysis. As shown in Table 6, the relative crystallinity index of cellulose powder was 60.83%, whereas those of the CNC samples prepared by mixed-acid hydrolysis ranged from 64.34% to 80.31%. The increase in relative crystallinity was primarily attributed to the preferential removal of less ordered cellulose regions during hydrolysis. The differences among the CNC samples indicate that the extent of removal of these regions depended on the hydrolysis conditions. The relative crystallinity index of SCNC was 79.72%. The values obtained for CNC-4 and CNC-5 were 80.31% and 78.52%, respectively, and were therefore comparable to that of SCNC. CNC-6, CNC-7, and CNC-8 exhibited lower relative crystallinity indices of 75.32%, 70.51%, and 64.34%, respectively. These results indicate that, under selected conditions, the CH_3COOH/H_2SO_4 mixed-acid system produced CNCs with relative crystallinity comparable to that obtained by conventional sulfuric acid hydrolysis, while using a substantially lower proportion of sulfuric acid in the reaction mixture.

Thermal degradation behavior of CNCs

Among the 9 orthogonal experimental runs, CNC-4 exhibited the highest measured yield, together with good aqueous dispersion stability and a high relative crystallinity index. It was therefore selected as the representative mixed-acid-hydrolyzed sample for comparison with SCNC. Figure 6 compares the TG curves of CNC-4 and SCNC. The mass-loss profiles of both samples can be broadly divided into three temperature regions.

Below approximately 150 °C, both samples exhibited a small mass loss, which was mainly attributed to the evaporation of physically adsorbed water. The similar mass losses in this temperature region indicate that CNC-4 and SCNC contained comparable amounts of removable moisture under the test conditions. The major mass loss occurred between approximately 150 and 350 °C, and was associated with dehydration, depolymerization, and decomposition of the cellulose chains. Compared with CNC-4, SCNC began to undergo substantial mass loss at a slightly lower temperature and exhibited a more rapid decrease in mass, indicating that CNC-4 had greater thermal resistance. This behavior is consistent with the catalytic effect of sulfate half-ester groups commonly introduced during sulfuric acid hydrolysis.[24] These acidic surface groups can promote dehydration and cleavage of cellulose chains during heating, thereby shifting thermal degradation toward lower temperatures.

Between approximately 350 and 800 °C, both samples exhibited slower mass loss associated with the further decomposition and carbonization of the remaining material. CNC-4 retained a slightly higher residual mass than SCNC at the end of the heating process. This difference may be related to variations in the surface chemistry and thermal degradation pathways of the two samples. However, the higher residual mass of CNC-4 cannot be attributed solely to differences in sulfur content or crystallinity without additional quantitative evidence. Overall, CNC-4 exhibited slightly greater thermal resistance than SCNC under the conditions examined, suggesting that the selected CH_3COOH/H_2SO_4 hydrolysis condition mitigated the thermal destabilization associated with conventional sulfuric acid hydrolysis.

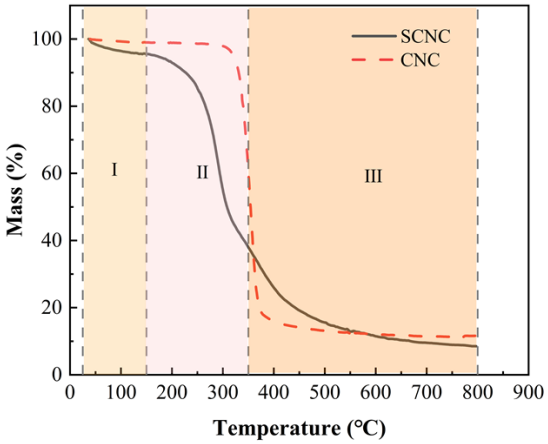


Figure 6: TG curves of CNC-4 and SCNC

CONCLUSION

In this study, cellulose nanocrystals were prepared from cellulose powder through CH_3COOH/H_2SO_4 mixed-acid hydrolysis. An L9(3^3) orthogonal experimental design was employed to evaluate the effects of the CH_3COOH/H_2SO_4 volume ratio, hydrolysis temperature, and hydrolysis time on the isolated CNC yield. Within the investigated factor levels, range analysis ranked the effects in the order of CH_3COOH/H_2SO_4 volume ratio, hydrolysis temperature, and hydrolysis time. The $A_2B_2C_3$ combination, corresponding to a CH_3COOH/H_2SO_4 volume ratio of 90:10, a hydrolysis temperature of 65 °C, and a hydrolysis time of 90 min, was selected on the basis of the range analysis. The additive main-effects model predicted an isolated CNC yield of 92.93%, whereas the confirmation experiment produced a yield of 87.90 ± 1.10% (n=3). The 5.03% difference between the predicted and experimental yields highlights a limitation of the L9(3^3) design as implemented in this study, because the additive main-effects model did not independently account for interactions among the investigated factors. This value was comparable to, but did not exceed, the 88.52% yield obtained for CNC-4 at 90:10, 55 °C, and 90 min. Accordingly, the preparation condition used for CNC-4 was regarded as the experimentally preferred condition within the range examined.

Mixed-acid hydrolysis converted the micrometer-scale cellulose powder into rod-like nanoscale particles with an average width of 50 ± 5 nm and an average length of 300 ± 50 nm. XRD analysis showed that the cellulose I crystalline structure was retained after hydrolysis. The relative crystallinity indices of the selected mixed-acid-derived CNC samples ranged from 64.34% to 80.31%, and the value obtained for CNC-4 (80.31%) was comparable to that of SCNC (79.72%). FTIR and XPS analyses supported the presence of carbonyl-containing ester groups and sulfur-containing surface species on CNC-4. Most mixed-acid-derived CNC suspensions exhibited substantial negative zeta potentials and remained visually stable after 15 days of standing, indicating favorable aqueous dispersion stability. CNC-4 exhibited slightly greater thermal resistance than SCNC under the conditions examined. However, the observed difference could not be assigned exclusively to sulfur content or crystallinity in the absence of additional quantitative evidence. Overall, the results demonstrate that selected CH_3COOH/H_2SO_4 hydrolysis conditions can produce CNCs with a high isolated yield, rod-like nanoscale morphology, favorable aqueous dispersion stability, and a high relative crystallinity index while using a lower proportion of sulfuric acid in the reaction medium than conventional sulfuric acid hydrolysis. These findings provide a systematic assessment of the relationships among mixed-acid hydrolysis conditions, isolated CNC yield, and physicochemical properties within the investigated experimental range.

Future studies will include independent replicate preparations under both the highest yielding tested condition and the condition selected by the range analysis. Critical process variables will be tightly controlled to assess batch-to-batch variability, and a more comprehensive experimental design will be employed to evaluate potential factor interactions. These efforts will allow a more rigorous assessment of the robustness and reproducibility of the mixed-acid hydrolysis process.

ACKNOWLEDGMENTS: This work was financially by National Natural Science Foundation of China (Grant Nos. 12362012, 12272189), Program for Innovative Research Team in Universities of Inner Mongolia Autonomous Region (Grant No. NMGIRT2402), The Basic Research Program Foundation of Institutions of Higher Education of Inner Mongolia (Grant Nos. JY20230103, JY20240069), Inner Mongolia Autonomous Region Higher Learning University Young Science and Technology Talents Development Project (NJYT23022), The Natural Science Foundation of Inner Mongolia (2024LHMS05034), Program of Inner Mongolia Autonomous Region Science and Technology Planning (2025SKJHZ0350), The Natural Science Foundation Key Project of Inner Mongolia Autonomous Region (2025ZD024).

REFERENCES

[1] Y. Habibi, L. A. Lucia and O. J. Rojas, *Chem. Rev.*, **110**, 3479 (2010), https://doi.org/10.1021/cr900339w
[2] E. J. Foster, R. J. Moon and U. P. Agarwal, *Chem. Soc. Rev.*, **47**, 2609 (2018), https://doi.org/10.1039/c6cs00895j
[3] M. Gao, Y. Shang and B. Li, *Green Chem.*, **24**, 9346 (2022), https://doi.org/10.1039/d2gc03003a
[4] P. Mali and A. P. Sherje, *Carbohyd. Polym.*, **275**, 118668 (2022), https://doi.org/10.1016/j.carbpol.2021.118668
[5] B. B. Kassie, M. J. Getahun and A. Azanaw, *Int. J. Biol. Macromol.*, **282**, 136949 (2024), https://doi.org/10.1016/j.ijbiomac.2024.136949
[6] S. P. Bangar, M. M. Harussani and R. A. Ilyas, *Food Hydrocoll.*, **130**, 107689 (2022), https://doi.org/10.1016/j.foodhyd.2022.107689
[7] W. Yang, Z. Mei and S. Feng, *ACS Sustain. Chem. Eng.*, **11**, 10172 (2023). https://doi.org/10.1021/acssuschemeng.3c02460
[8] D. Bondeson, A. Mathew and K. Oksman, *Cellulose*, **13**, 171 (2006), https://doi.org/10.1007/s10570-006-9061-4
[9] S. Beck-Candanedo, M. Roman and D. G. Gray, *Biomacromolecules*, **6**, 1048 (2005), https://doi.org/10.1021/bm049300p
[10] L. Chen, Q. Wang and K. Hirth, *Cellulose*, **22**, 1753 (2015), https://doi.org/10.1007/s10570-015-0615-1
[11] L. Chen, J. Y. Zhu and C. Baez, *Green Chem.*, **18**, 3835 (2016), https://doi.org/10.1039/c6gc00687f
[12] M. Roman and W. T. Winter, *Biomacromolecules*, **5**, 1671 (2004), https://doi.org/10.1021/bm034519+
[13] X. Yang, Y. Chen and C. Zhang, *Compos. Part B: Eng.*, **249**, 110386 (2023), https://doi.org/10.1016/j.compositesb.2022.110386
[14] B. Wang, S. Qiu and Z. Chen, *Carbohyd. Polym.*, **299**, 120008 (2023), https://doi.org/10.1016/j.carbpol.2022.120008
[15] H. Wang, M. Zhang and J. Hu, *Carbohyd. Polym.*, **297**, 120062 (2022), https://doi.org/10.1016/j.carbpol.2022.120062
[16] A. Najahi, M. Delgado-Aguilar and J. L. Putaux, *Biomacromolecules*, **26**, 1372 (2025), https://doi.org/10.1021/acs.biomac.4c01737
[17] S. C. Espinosa, T. Kuhnt and E. J. Foster, *Biomacromolecules*, **14**, 1223 (2013), https://doi.org/10.1021/bm400219u
[18] H. Du, C. Liu and X. Mu, *Cellulose*, **23**, 2389 (2016), https://doi.org/10.1007/s10570-016-0963-5
[19] M. Cheng, Z. Qin and J. Hu, *Carbohyd. Polym.*, **231**, 115701 (2020), https://doi.org/10.1016/j.carbpol.2019.115701
[20] H. Xie, Z. Zou and H. Du, *Carbohyd. Polym.*, **223**, 115116 (2019), https://doi.org/10.1016/j.carbpol.2019.115116
[21] H. Wang, H. Xie and H. Du, *Carbohyd. Polym.*, **239**, 116233 (2020), https://doi.org/10.1016/j.carbpol.2020.116233
[22] C. S. Rubi, J. U. Prakash and S. J. Juliyana, *Sci. Eng. Compos. Mater.*, **31** (2024), https://doi.org/10.1515/secm-2024-0008
[23] V. Grachev, S. Lombardo and C. Bartic, *Carbohyd. Polym.*, **333**, 121949 (2024), https://doi.org/10.1016/j.carbpol.2024.121949
[24] F. D. Acierno, C. A. Michal and M. J. MacLachlan, *Chem. Rev.*, **123**, 7295 (2023), https://doi.org/10.1021/acs.chemrev.2c00816
[25] L. Xing, C. Hu and W. Zhang, *Carbohyd. Polym.*, **229**, 115539 (2020), https://doi.org/10.1016/j.carbpol.2019.115539
[26] Z. Wang, H. Wang and X. Pan, *Ind. Crop. Prod.*, **214**, 118575 (2024), https://doi.org/10.1016/j.indcrop.2024.118575